

HIGH-ENERGY X-RAY PINHOLE CAMERA FOR HIGH-RESOLUTION ELECTRON
BEAM SIZE MEASUREMENTS *

B. Yang, J. Morgan, S.H. Lee and H. Shang

To be presented at the 2016 International Beam Instrumentation Conference IBIC 2016
September 11-15, 2016

The submitted manuscript has been created by UChicago Argonne, LLC, Operator of Argonne National Laboratory ("Argonne"). Argonne, a U.S. Department of Energy Office of Science laboratory, is operated under Contract No. DE-AC02-06CH11357. The U.S. Government retains for itself, and others acting on its behalf, a paid-up nonexclusive, irrevocable worldwide license in said article to reproduce, prepare derivative works, distribute copies to the public, and perform publicly and display publicly, by or on behalf of the Government. The Department of Energy will provide public access to these results of federally sponsored research in accordance with the DOE Public Access Plan. <http://energy.gov/downloads/doe-public-access-plan>.

*Work supported by the U.S. Department of Energy, Office of Science, under Contract No. DE-AC02-06CH11357.

HIGH-ENERGY X-RAY PINHOLE CAMERA FOR HIGH-RESOLUTION ELECTRON BEAM SIZE MEASUREMENTS*

B. Yang, J. Morgan, S.H. Lee and H. Shang

Advanced Photon Source, Argonne National Laboratory, Argonne, IL 60439 USA

Abstract

The Advanced Photon Source (APS) is developing a multi-bend achromat (MBA) lattice based storage ring as the next major upgrade, featuring a 20-fold reduction in emittance. Combining the reduction of beta functions, the electron beam sizes at bend magnet sources may be reduced to reach 5 – 10 μm for 10% vertical coupling. The x-ray pinhole camera currently used for beam size monitoring will not be adequate for the new task. By increasing the operating photon energy to 120 – 200 keV, the pinhole camera's resolution is expected to reach below 4 μm . The peak height of the pinhole image will be used to monitor relative changes of the beam sizes and enable the feedback control of the emittance. We present the simulation and the design of a beam size monitor for the APS storage ring.

INTRODUCTION

A new generation of storage-ring based synchrotron radiation sources using multi-bend achromat (MBA) lattices are being planned, designed, constructed, and commissioned worldwide [1,2]. These rings are expected to operate with total emittance two-orders of magnitude lower than many of the third-generation synchrotron radiation sources. Table 1 lists the expected beam sizes at the bend magnet sources after the APS Upgrade (APS-U) at 66 pm total emittance. Due to small beta functions inherent to the MBA lattices, the electron beam sizes in these rings are in the micrometre range, with the potential of reaching sub-micrometre level for vertical couplings under 1%. Robust and accurate diagnostics for these minute beam sizes are important for the operations of these new sources.

In this work, we will discuss the plans and design of the beam size monitor (BSM) for the APS-U MBA storage ring. We will cover the simulated performance of the high-energy x-ray pinhole camera, conceptual design, and alternative techniques to be implemented in parallel.

Table 1: Expected e-beam sizes for APS-U storage ring

Plane	Horizontal		Vertical	
Beta function	1.8 m		3.9 m	
Vertical coupling	Full	10%	Full	10%
Beam size (μm)	7.8	10.4	11.3	5.0

COMPUTER SIMULATION

Pinhole images can be modelled using the well-known Fresnel diffraction algorithm. At wavelength λ , the photon intensity at the image plane can be expressed as, $I_0(x') = |A(x')|^2$ where the photon wave amplitude is

$$A(x') = \frac{A'_0}{1+i} \left[F\left(\sqrt{\frac{2}{\lambda f}}\left(f\varphi + \frac{d}{2}\right)\right) - F\left(\sqrt{\frac{2}{\lambda f}}\left(f\varphi - \frac{d}{2}\right)\right) \right]. \quad (1)$$

The length parameter f is given by $1/f = 1/S + 1/S'$, where S is the distance from the source to the pinhole, S' is the distance from the pinhole to the image plane. Furthermore, $\varphi = x'/S'$, d is the total width of the pinhole slit, A'_0 is an amplitude constant, and the complex Fresnel integral is defined as

$$F(x) = C(x) + iS(x) = \int_0^x e^{i\pi t^2/2} dt. \quad (2)$$

If we map the image coordinates x' back to the source plane coordinates x using the optical magnification of the beamline, $x = x'/M = x'S/S'$, the intensity at the mapped source can be obtained simply by using $\varphi = x/S$ and a different amplitude constant in Eq. (1). Finally, for finite source sizes, the calculated intensity distribution needs to be convolved with the source distribution. The program *sddsfresnel* implements these algorithms and can be used to calculate the one-dimensional Fresnel profile for a given geometry and a given source size.

For the perspective APS bend magnet beamline with $S = 8.5$ m, $S' = 11.5$ m, numerical calculation shows that the resolution of the pinhole camera is near optimal for slits width of 10- μm for photon energy of 120 keV. Figure 1 shows the normalized diffraction profiles from such a pinhole with source sizes ranging from 0 to 20 μm . We can see that the profiles can be clearly resolved down to 5 μm , but not below 3 μm . Since photons with energy of 100 – 500 keV are often referred to as soft gamma rays, this work is about soft gamma ray pinhole camera techniques.

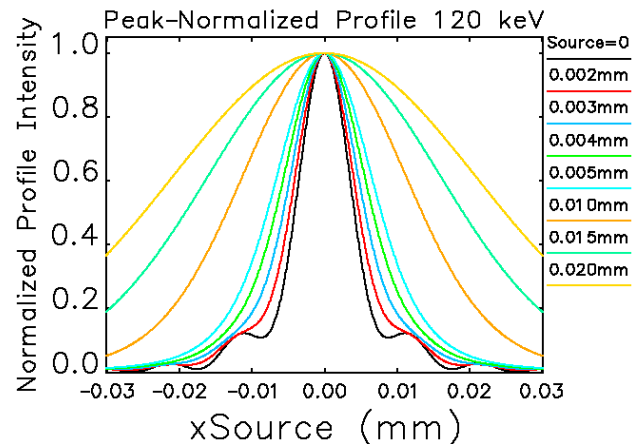


Figure 1: Fresnel diffraction profile using monochromatic 120 keV x-ray photons for zero source size; and convolution with Gaussian source with rms width of 2 – 20 μm . All profiles are normalized at the peak for easy comparison.

* Work supported by U.S. Department of Energy, Office of Science, under Contract No. DE-AC02-06CH11357.

BEAMLINE DESIGN

Source

The APS-U beam size monitor will use one or more bend magnet (BM) sources where a three-pole wiggler (3PW) may be installed. The peak field of an APS-U 3PW is 1.17 T. At ± 0.5 mrad from optical axis, the effective field is approximately 1.0 T. Figure 2 shows the x-ray flux through a 10- μm square pinhole at 8.5 m from the sources. The 3PW is highly desirable since it generates 10 – 200 times more photons in 100 – 200 keV region than the APS-U BM sources with 0.55 – 0.61 T field.

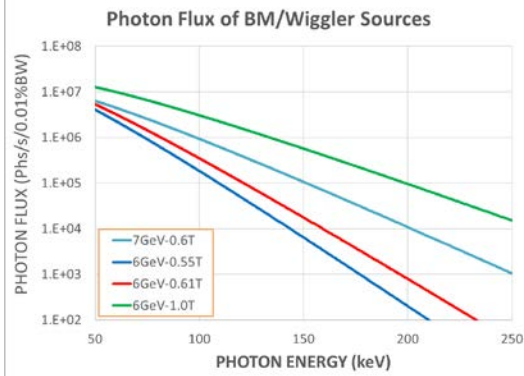


Figure 2: Spectral photon flux through a 10 μm square pinhole at 8.5 m from an APS-U bend magnet/wiggler source. The electron beam is 6-GeV in energy at 200 mA. Pinhole flux for the current APS source (7GeV/100mA) is shown for comparison.

Pinhole Slits

Since the x-ray beam at 8 m from the source is wider than the 10- μm pinhole width, it is estimated that in order to reduce the background of profile measurements to under 1% of the peak counts, the blade transmission needs to be less than 0.1%. Figure 3 plots the transmission efficiency of 3 – 6 mm tantalum and tungsten blades. We can see that The useable photon energy is 155 – 165 keV for 3-mm Ta and W blades, and 210 keV for 5-mm W or 6-mm Ta blades.

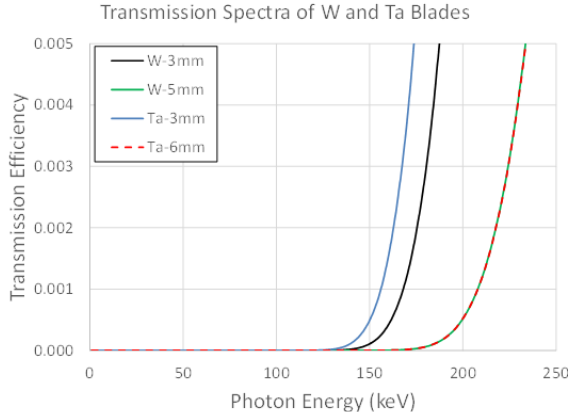


Figure 3: Transmission spectrum of tungsten (3 mm and 5 mm) and tantalum (3 mm and 6 mm) blades.

Detectors

At 4:3 magnification, the entire diffraction profile has a FWHM around 20 μm and required spatial resolution of the detector needs to be 2 μm RMS or better. This spec is difficult for commonly used scintillation screens in x-ray pinhole cameras: to obtain required spatial resolution, the screen thickness should be 10's of μm or less, which results in very low efficiency for high-energy photons. We propose to use 5- μm slits to define the spatial resolution, after which a monochromator and efficient detector can be used. Simulation shows that the slit will not broaden the image peak significantly. However, it does make it difficult to measure horizontal and vertical profiles in a same setup. We will build two beamlines side-by-side for measuring horizontal and vertical beam sizes separately.

To select the desired photon energy, we propose to use single crystal monochromators. Table 2 lists the properties of selected crystals and Figure 4 shows proposed optics design. We note that a larger deflection angle (2θ) makes it easier for the beam dump to block the white x-ray beam from reaching the detector and to reduce the background counts. While many semiconductor and scintillator detectors have nearly 100% efficiency for x-ray photons below 200 keV, the highly concentrated dose in a small region of 10 – 20 microns in radius may destroy the detectors locally and degrade its efficiency quickly. Gaseous ion chambers will be used to avoid localized radiation damage.

Table 2: Property of a few selected crystals

Crystal	Si(111)	Ge (111)	Ge (220)
Bandwidth $\Delta E/E (10^{-4})$	1.31	3.41	1.57
2θ at 120 keV	1.89°	1.81°	2.96°
2θ at 200 keV	1.13°	1.09°	1.78 °

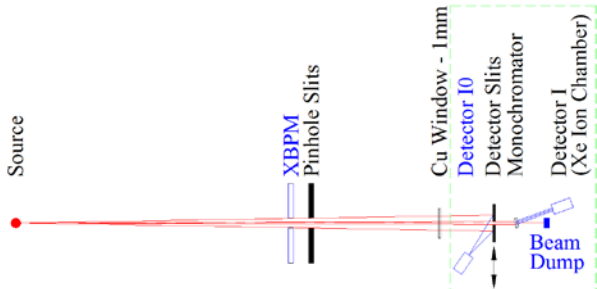


Figure 4: Soft-gamma-ray pinhole camera detector using a crystal monochromator.

Table 3 summaries the key design parameters of the APS-U soft gamma ray pinhole camera. We will keep the optical transport in vacuum until the detector slits. This approach has two advantages: (1) The narrow slits will be kept in vacuum and will not be oxidized or contaminated in air. (2) Scattering effect from the window will be minimized at the detector due to the short distance between the two.

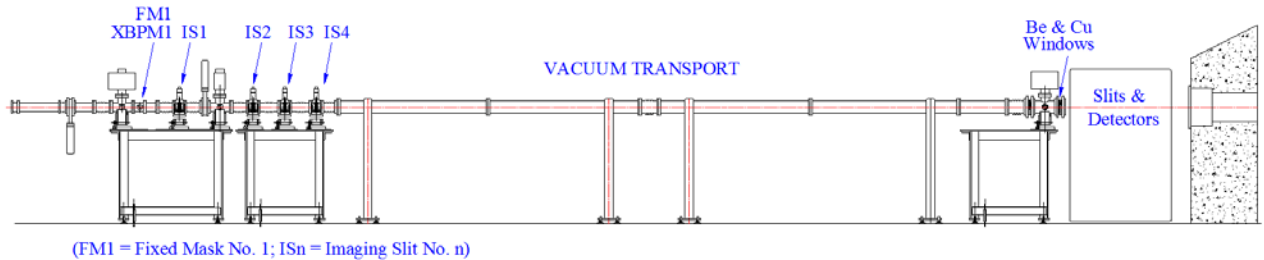


Figure 5: Beamlne layout.

Table 3: APS-U beam size monitor design parameters

Photon energy	120 keV	200 keV
Source distance	8.5 m	
Detector distance	11.5 m	
Imaging slit width	10×500μm	8×500 μm
Detector slit width	5×100 μm	4×100 μm
Absorption of 20 cm Xe	13%	4%
Source size range	> 5 μm	> 4 μm

Beamlne layout

Figure 5 shows the beam size monitor beamline which will be contained entirely in the accelerator tunnel in one of the unused bend magnet front ends. The beamline is divided into four functional branch lines by the first fixed mask. Table 4 lists these branch lines: The first branch line (BL1) uses the upstream bend magnet source to measure the e-beam angle and position so the orbit feedback control system can keep the beam centred on the optics and detectors of the BSM. The second and the third beamlines (BL2 and BL3) uses the 3PW source to measure the horizontal and vertical e-beam size. The fourth branch line (BL4) uses the downstream BM source and x-ray diffraction from selected apertures for photon energy in 6 – 12 keV range.

Table 4: APS-U beam size monitor branch lines

Branch line	Measurements functions
1. XBPM	Beam angle and source position
2. Horizontal	Horizontal γ-pinhole camera
3. Vertical	Vertical γ-pinhole camera
4. X-ray diffraction	Fresnel diffraction pattern

In this beamline, the first fixed mask (FM1) is the only component with power load over 100 W. Its main body, including the absorber and the two flanges will be machined from a solid piece of CuCrZr similar to those tested recently in NSLS II [3]. Figure 6 shows the thermal analysis of this mask. For normal operations with the current APS bend magnet source in the test beamline, the maximum temperature is 61°C and the maximum von Mises stress is 100 MPa. At the worst missteering, the temperature increases to 64° C and the stress to 152 MPa. In both cases, the mask operates well within the safe operating region of the material. The analysis for FM1 with 3PW source is in progress, which is expected to result in minor adjustments in the mask design.

MODE OF OPERATION

Absolute beam size measurements

The basic operation mode of the beamline is absolute beam size measurements, i.e., horizontal and vertical beam profile measurements. In this mode, the detector slits are scanned horizontally in BL2 and vertically in BL3. Figure 7 shows the simulated beam profiles from these measurements, where the effects of the detector slits width are taken into account.

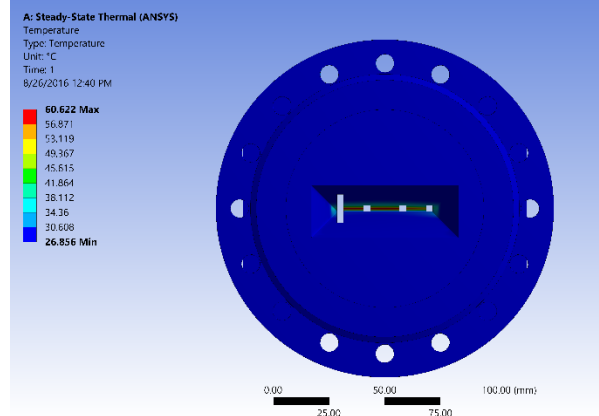


Figure 6: Thermal analysis of the first fixed mask which divides the APS BM beam into four branch beamlines.

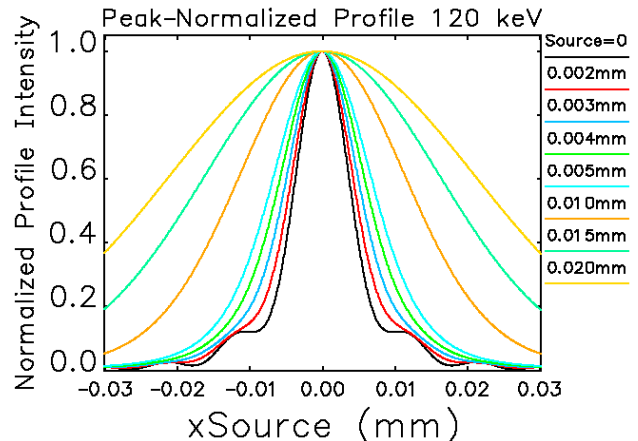


Figure 7: Calculated photon beam intensity profiles using monochromatic 120 keV x-rays for source size of 0 – 20 μm. The imaging and detector slits are 10 μm and 5 μm wide, respectively.

Relative beam size measurements

To stabilize beam size / emittance during user operations or experimentally minimize vertical couplings, it is desirable to have faster data stream reflecting beam size changes in real time for feedback controls. If we place the detector slits at the diffraction peaks in BL2 and BL3, the intensity ratio of the two detector signals (I, I_0) is directly correlated with e-beam sizes. Figure 8 shows the ratio I_0/I as a function of the beam size for detector slits of 2 – 12 μm . We can make several observations from the plot:

- The intensity ratios are sensitive to the source size change. For example, for $\pm 10\%$ size change near 10 μm , the intensity ratio changes $\pm 7.7\%$. On the other hand, it is not very sensitive to the detector slit width until the beam size is below 5 μm .
- For any given slit width, the intensity ratio is reasonably sensitive to beam size changes down to 2- μm level.
- The beam size range of 2 – 25 μm covers the planned user operations with ample margins. If the curve in Figure 8 is properly calibrated at two beam sizes between 10 μm to 25 μm , the intensity ratio can even be used as an absolute beam size data with usable accuracy.
- If the detector slit is not at the peak due to beam motion (see Figure 7), the signal drop from I -detector can be misconstrued as an increase in beam size. To avoid this problem: (A) a good XBPM system at BL1 is important for keeping the two pinholes aligned with the source; and (B) a wider slit is usually more favourable since it is less sensitive to the beam motion.

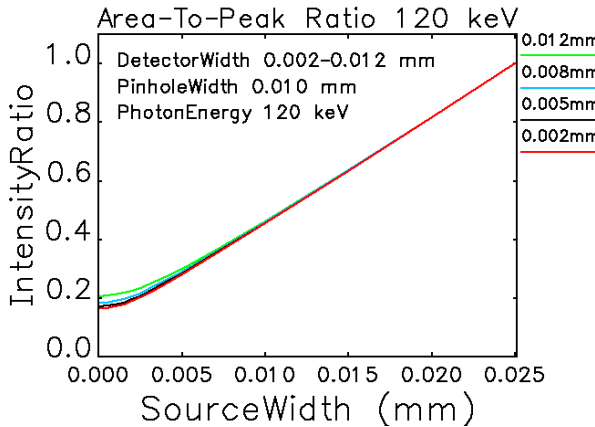


Figure 8: The normalized intensity ratio $R=I_0/I$ for three different pinhole aperture sizes at 120 keV photon energy.

ALTERNATIVE TECHNIQUE

While the soft gamma ray pinhole cameras have sufficient resolution for measuring nominal beam sizes in user operations, future machine development may produce beam sizes below 4 μm and require diagnostics with better resolution. From Figure 7, we see that for small beam sizes in 1 – 4 μm range, the diffraction profile is most sensitive to source size change in the skirt region, around the first and second minima. We can take advantage of this feature and push the working range of the soft gamma ray pinhole

to 1- μm level, provided we can maintain a good signal-to-noise ratio for the pinhole camera.

An alternative approach is to build an x-ray diffraction line in BL4, and install an optical aperture at ~ 9 m location and measure the monochromatic diffraction image at 20 m mark. Using a square optical aperture, the diffraction pattern will be sensitive to the beam sizes down to several micrometres at 8 keV x-ray energy [4]. Using a pair of Young's double slits as the optical aperture will offer even higher beam size sensitivity. Figure 9 shows diffraction patterns at 8 keV from a mask with two 10- μm slits separated by 80 μm . The pattern is very sensitive to source size change between 1 – 5 μm region.

CONCLUSION

Fresnel diffraction calculation shows that a soft gamma ray pinhole camera (120 – 200 keV) using an imaging slit and a detector slit will be able to resolve electron beam sizes down to 3 – 4 μm level in one-dimensional profile measurements. When the two slits are both centered on the optical axis, the transmitted gamma ray flux provides a fast, but less accurate measurement on beam sizes down to 2- μm level. The conceptual design of the APS-U beam size monitor is based on these simulations and is expected to fulfil the requirements of the APS Upgrade. An additional branch line will be allocated for x-ray diffraction measurements, as an assurance for meeting resolution specifications and also as an option for future upgrade.

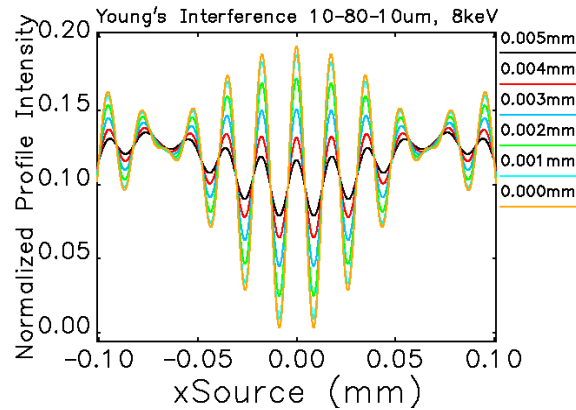


Figure 9: 8-keV x-ray diffraction pattern from Young's double slits of 80 μm spacing with source and image distances of 9 m and 11 m respectively.

REFERENCES

- [1] R. Hettel, DLSR design and plans: an international overview, *J. Synchrotron Rad.* 21, pp. 843-855 (2014).
- [2] M. Borland, V. Sajaev, Y. Sun, A. Xiao, Hybrid Seven-Bend-Achromat Lattice for the Advanced Photon Source Upgrade, *IPAC 2015*, pp. 1776 – 1779 (2015).
- [3] S. Sharma, "A novel design of high power masks and slits," *MEDSI* (2014).
- [4] M. Masaki, Y. Shimosaki, S. Takano, M. Takao, "Novel emittance diagnostics for diffraction limited light sources based on x-ray Fresnel diffractometry," *IBIC* (2014), 274 - 278.